COTS-Based Stick-on Electricity Meters for Building Submetering

Michael C. Lorek, *Student Member, IEEE,* Fabien Chraim, *Student Member, IEEE,*
Kristofer S.J. Pister, Steven Lanzisera, *Member, IEEE*

***Abstract*—We demonstrate a low-cost, 19 x 12 mm prototype Peel-and-Stick Electricity Meter (PASEM) PCB to replace traditional in-circuit-breaker-panel current and voltage sensors for building submetering. PASEM sensors are installed on the external face of circuit breakers to generate voltage and current signals at a 1920 Hz sample rate. This allows for the computation of real and apparent power as well as capturing harmonics created by non-linear loads. The prototype sensor is built using commercially available components, resulting in a component cost of under $10 per PASEM in moderate quantities. With no high-voltage install work requiring an electrician, this leads to an installed system cost that is roughly ten times lower than traditional submetering technology. Measurement results from lab characterization as well as a real-world residential dwelling installation are presented, verifying the operation of our proposed PASEM sensor. The PASEM sensor can resolve breaker power levels below 10W and consumes approximately 16 mA from a 5V supply.**

***Index Terms*—Building submetering, circuit breaker, electricity meter, energy meter, power meter, smart building.**

I. Introduction

ELECTRICITY usage in the USA is responsible for 40% of our primary energy expenditure and carbon emissions [1]. Commercial buildings research shows that electricity submetering combined with data analytics and maintenance follow-up can reduce a building's electricity use by 10% to 30% [2]–[5]; it is very likely that similar energy savings can be achieved in industrial (and possibly residential) environments. However, very few buildings are outfitted with the meters required to enable these savings because of the high cost of installation. In order to enable the worldwide reduction of building electricity usage, it is critical to develop electricity metering technologies that provide more granular energy information with dramatically reduced install costs.

An earlier version of this paper was presented at the IEEE SENSORS 2013 Conference and published in its Proceedings.

M. Lorek, F. Chraim, and K.S.J. Pister are with the Berkeley Sensor and Actuator Center, University of California, Berkeley, CA 94720 USA (e-mail: mlorek@eecs.berkeley.edu, chraim@eecs.berkeley.edu, pister@eecs.berkeley.edu).

S. Lanzisera is with the Environmental Energy Technologies Division, Lawrence Berkeley National Laboratory, Berkeley, CA 94720 USA (e-mail: smlanzisera@lbl.gov).

This work was supported by the Assistant Secretary for Energy Efficiency and Renewable Energy, Building Technologies Program, of the U.S. Department of Energy, under Contract No. DE-AC02-05CH11231.

Manuscript received ##; revised ##.

Color versions of one or more of the figures in this paper are available online at http://ieeexplore.ieee.org.

Today's commercially available circuit breaker panel submetering technologies require bulky current transformers (CTs) and voltage connections to be installed inside the panel; a photo of a traditional submetering installation is shown in Figure 1a, and a wiring diagram of the system in Figure 1b. To install a system such as this, an electrician must either shut down the building's power or perform dangerous hot work on the panel. The installer must open the electrical panel and spend significant time to install metering components, as well as external conduit and enclosures to cover the equipment and signal leads. The total insallation cost is subsequently dominated by the labor required to carefully install all hardware, conduit, and wiring by highly-skilled tradespeople, while also adhering to safety and building code requirements [4], [5]. This results in an installed cost that is approximately $\$1,500 - \$5,000$ per panel. Thus, a typical mid-size, mid-life commercial building requiring several tens of metering points can cost up to $100,000 for three-phase submetering, resulting in a payback period in excess of ten years. Therefore, a great need exists for a circuit breaker panel submetering system that can be installed without an electrician for minimal time and money investment.

To meet these goals, it has been proposed to replace the in-panel hardware with non-contact-based sensor devices on the outside of the circuit breakers. This provides a number of benefits. First, installation on the outside of the circuit breaker panel does not require an electrician. Second, since the system is self-contained on the exterior panel face, no external wiring or conduit must be installed. While non-contact-based energy meters have previously been presented in the literature, they suffer from multiple drawbacks that make widespread deployment difficult, and limit the practical value of the data that is acquired. Multiple works have shown current magnitude sensors based on a custom MEMS process, but these systems do not sense the line voltage and, thus, cannot calculate real power dissipation [6]–[9]. Many of these systems also have low sampling rates that don't perform well with non-linear loads, and prevent the ability to detect and diagnose load faults by examining the spectral content of the acquired signals. In [10], a 1 kHz current signal sample rate is reported, however the sensor itself is too large to submeter individual circuit breakers, and the system has difficulty dealing with multi-phase power systems.

In this paper, we present the design of a Peel-and-Stick Electricity Meter (PASEM) sensor PCB built using Commercial Off-The-Shelf (COTS) components, in a 19 x 12 mm form factor suitable for metering individual circuit breakers.

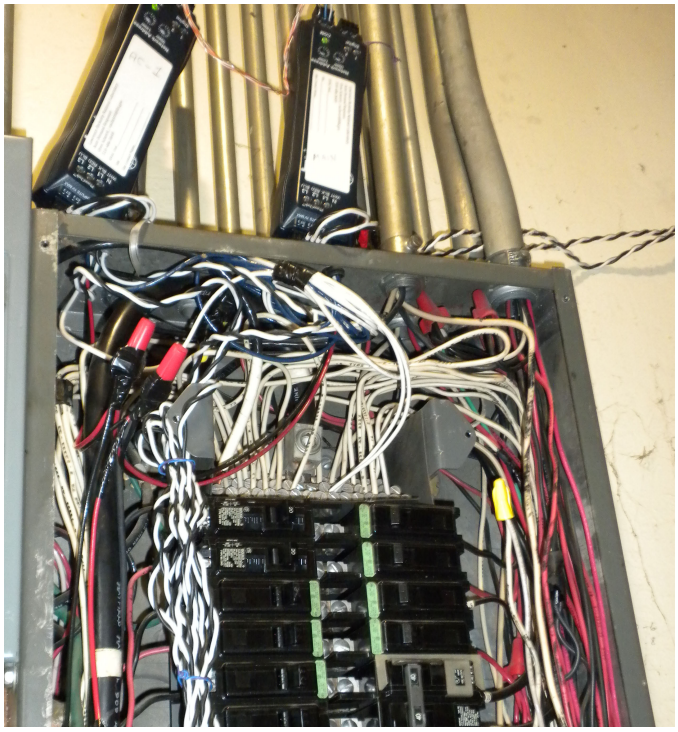

(a)

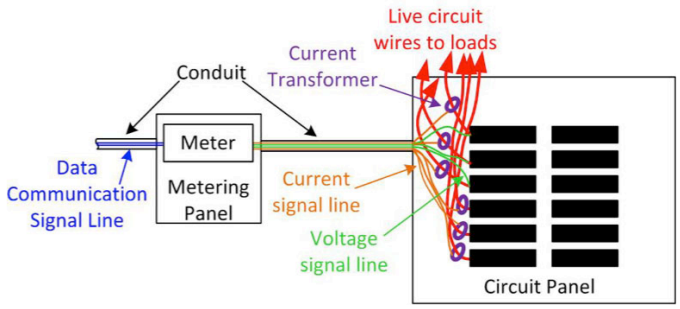

(b)

Fig. 1. (a) Traditional current-transformer-based panel submeter installation. (b) Wiring diagram showing voltage and current measurement signal lines.

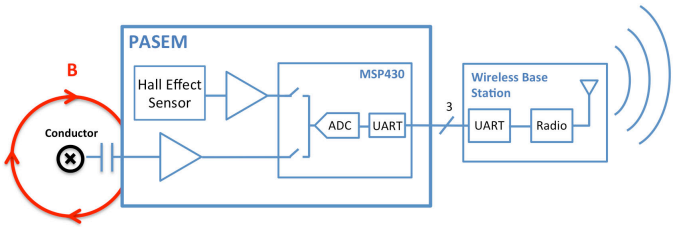

Fig. 2. PASEM system block diagram showing sensing techniques, PASEM, and wireless base station.

We believe that an PASEM design based on commercially available components is practical for widespread adoption due to its standard PCB fabrication and assembly requirements. Our sensor measures a circuit breaker's current *and* voltage with a 1 kHz analog front end bandwidth and 1920 Hz sampling rate. The system shows very good measurement performance and the PASEM can be built for a component cost below $10 in moderate quantities.

Fig. 3. PASEM system installation on circuit breaker panel. Five PASEM devices installed with wireless base station at bottom. Circuit breakers labeled for reference.

II. System Overview

In this section, an overview of each panel submetering hardware subsystem and the flow of sensor data will be discussed. A block diagram of the in-panel system can be seen in Figure 2, and a photo of a real installation in our lab with five metered breakers can be seen in Figure 3. The entire system is powered by one standard AC-DC converter plugged into a nearby power outlet.

A. PASEM Board

Each PASEM sensor board is equipped with an analog front end for current and voltage signal conditioning, as well as a Texas Instruments MSP430G2131 microcontroller. Details of the sensing and analog circuits will be discussed in Section III. The entire PASEM board consumes around 16 mA from a 5V supply. A close-up image of the 19 x 12 mm assembled PASEM PCB board can be seen in Figure 4. The cost breakdown of the components on the PASEM PCB is shown in Table I, quoted from large electronic component distributors for a quantity of 100 PASEM boards.

The PASEM's microcontroller is used for two purposes in our system: sampling the analog voltage and current sense

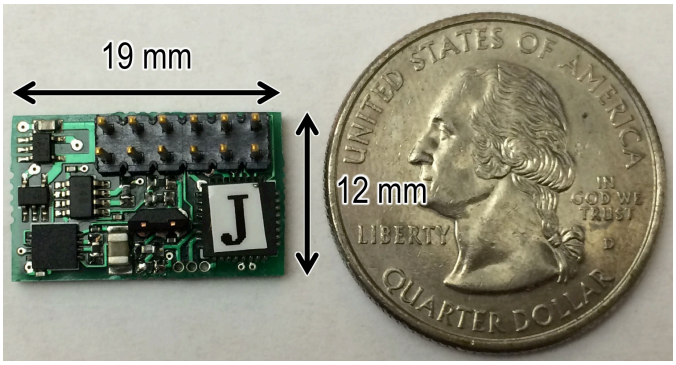

Fig. 4. Assembled Peel-and-Stick Electricity Meter with US quarter dollar coin for size reference.

PASEM Component	Cost
Microcontroller	$1.13
2x Amplifier ICs	$3.21
2x Linear Voltage Regulator ICs	$1.14
Hall Effect Sensor	$1.04
Passives	$1.83
2x6 Header Block	$1.05
Total	**$9.40**

TABLE I
SIMPLIFIED BILL OF MATERIALS FOR PASEM BOARD

signals, and transmitting samples to the wireless base station via a wired bus. To preserve information in the harmonics of the sensed current signals, a 1920 Hz sampling rate is used in the 10-bit microcontroller ADC. This sampling frequency was selected because it is a power-of-two multiple of the 60Hz fundamental line frequency, enabling straightforward computation of the fast Fourier transform (FFT) without aliasing. Thirty two samples (one 60 Hz cycle) of both the voltage and current sense signals are stored in the microcontroller's memory at all times. Acting as a Serial Peripheral Interface (SPI) bus slave, the PASEM's SPI interface clock is provided by the wireless mote base station. When the PASEM microcontroller gets a request for data from the wireless mote, the stored samples are transmitted to the base station over the SPI bus at a 500 kHz clock rate.

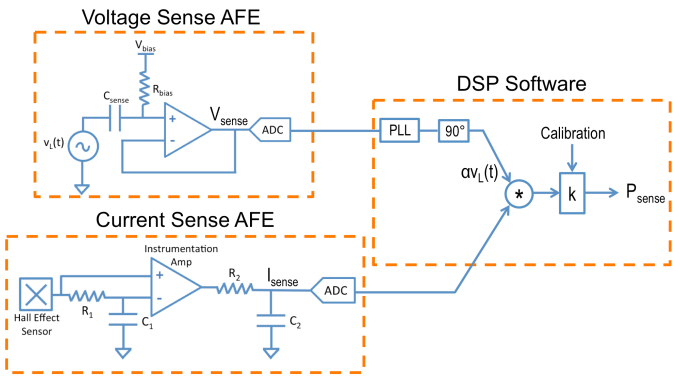

Fig. 5. Signal processing block diagram showing current and voltage analog sensing circuits, and DSP real power calculation technique.

B. Wireless Base Station

In this system, a Raspberry Pi with custom adapter board functions as a base station for PASEM devices installed on the breaker panel. As an SPI master, the wireless base station device requests data from an PASEM sensor over SPI and provides a clock for the SPI bus. Voltage and current samples from the SEMs are received by the wireless mote over the wired bus, and subsequently transmitted to a computer for further processing.

C. Laptop Computer

A laptop receives wireless data transmissions from the breaker panel wireless base station, and also performs subsequent DSP computations on the received samples. Python scripts are executed on the laptop that unpack the PASEM signals, calculate parameters of interest, such as the metered breakers' line voltage signal and real power usage, and report the data to a cloud-based Simple Measurement and Actuation Profile (sMAP) server [11] for convenient viewing.

III. SENSING IMPLEMENTATION

A. Voltage Sensing

The analog circuits used for our capacitive voltage sensing scheme can be seen in Figure 5. The sense capacitance is essentially a parallel-plate capacitor formed between the bottom metal plane of the PASEM board and the conductor in the circuit breaker. For large capacitive coupling, careful PASEM board layout consideration was practiced to keep the bottom layer densely filled with metal. Assuming the sense capacitance remains constant, the capacitor current can be monitored to obtain the time-derivative of the breaker's line voltage: $\frac{dv_L(t)}{dt} = \frac{i_{sense}}{C_{sense}}$. The amplitude of this signal is controlled by the value of R_{bias} and is buffered with an opamp to drive the ADC input.

B. Current Sensing

At the heart of our current sensing scheme is a hall effect sensor that detects magnetic fields generated by currents flowing through a metered circuit breaker. The sensor used in this work is an SIP package A1301 Hall Effect Sensor by Allegro MicroSystems, with a 2.5 mV/Gauss sensitivity. A diagram of the current sensing analog circuitry is shown in Figure 5. Since the output of the hall effect sensor is single-ended, a reference needs to be generated for the instrumentation amplifier's inverting input. To create this reference, the output of the hall effect sensor is averaged by the $f_p \approx 0.3$ Hz R_1C_1 low-pass filter ($R_1 = 10k\Omega, C_1 = 47\mu F$). The amplified current sense signal is then passed through the $f_p \approx 1$ kHz R_2C_2 ($R_2 = 16\Omega, C_2 = 10\mu F$) anti-aliasing filter and is sampled at 1920 Hz by the microcontroller's ADC.

C. Real Power Estimation

Figure 5 outlines our technique used to estimate real power once a circuit breaker's I_{sense} and V_{sense} ($\frac{dv_L(t)}{dt}$) signals are obtained in the digital domain. To calculate real power,

a signal representing the circuit's line voltage, $v_L(t)$, must be determined. Assuming that $v_L(t)$ is sinusoidal, shifting the phase of the measured V_{sense} signal by 90° is analagous to integration. We have created a software phase-locked loop in Python that tracks the phase of the V_{sense} signal, and synthesizes an ideal sinusoid with phase matched to $v_L(t)$, shown as $\alpha v_L(t)$ in Figure 5. Example measured I_{sense}, V_{sense} , and $\alpha v_L(t)$ signals can be seen in Figure 9a.

To calculate the instantaneous power waveform, $\alpha v_L(t)$ and I_{sense} are multiplied together. The mean of this instantaneous power signal provides an estimate of the real power dissipated in the circuit, in arbitrary units. A calibration constant must be found to map the power output of our system to real power in Watts. This calibration constant can be found by applying a known load to a submetered circuit while monitoring the software DSP real power estimator output. Assuming the PASEM boards' analog circuits are well matched and the sensors can be placed in the same location on identical breakers, the calibration routine must only be performed once for every type of breaker to be metered. Once the calibration factors are determined, they are programmed into the laptop's python script for real-time data logging in Watts.

IV. Experimental Results

In the characterization of our PASEM prototype, measurements were completed in a laboratory environment as well as in an actual residential installation. Figure 6a shows the internals of a common residential circuit breaker with a bimetallic strip trip mechanism. When the current through the breaker is large enough, the heat dissipated in the bimetallic strip causes a deflection that breaks the circuit. A second common type of circuit breaker, which functions fundamentally differently, is shown in Figure 6b. The solenoid in the circuit breaker concentrates the magnetic field in its surroundings, attributing to a Lorentz force on nearby conductors. As current increases past the breaker's rated limit, the electromagnetic force is large enough to actuate the breaker. It is important to note that the breakers tested in this work do not contain solenoids, which would increase the magnetic field magnitude around the breaker by 10-20x. If solenoidal breakers were to be considered, the design of a high resolution current sensing system would be much easier due to the drastically increased signal-to-noise ratio (SNR). For this work, we focused on the more challenging but also much more prevalent, thermally (thermal-magnetic) actuated circuit breakers. From our investigations, most thermal and thermal-magnetic breakers have internal geometries and current paths that are very similar to Figure 6a.

A. Evaluation of Real Power Estimation Accuracy

To characterize the real power estimation performance of our PASEM sensor, its voltage and current sense outputs were monitored across a wide range of load currents; the test setup will now be described in detail. Our PASEM device was powered by a 5V DC power supply and mounted onto the face of a circuit breaker in a bench top circuit breaker panel. The bench top panel is powered with a standard US power plug,

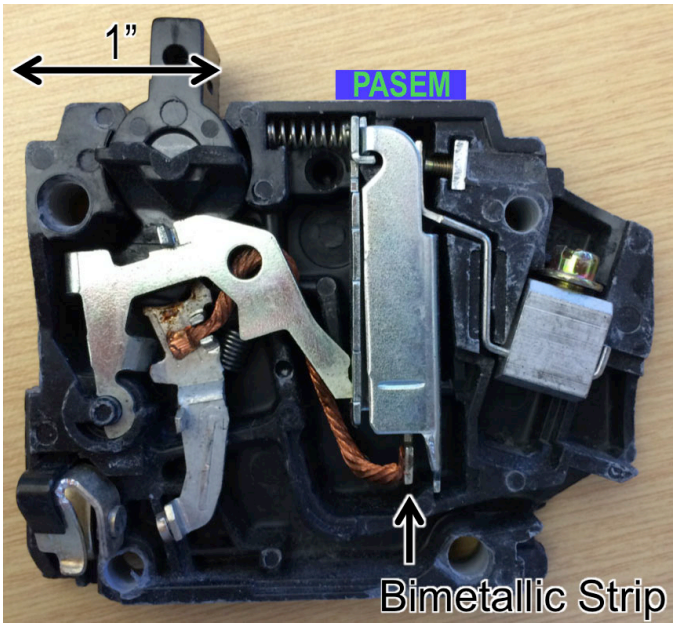

(a)

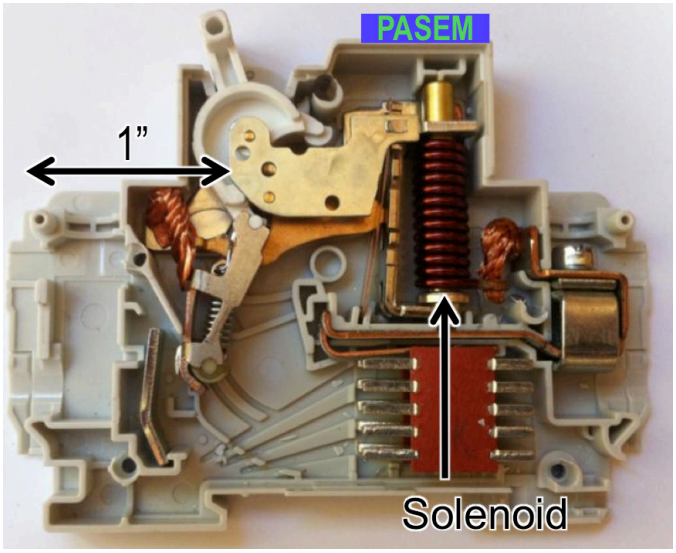

(b)

Fig. 6. (a) Thermal-actuated circuit breaker innards with bimetallic strip and PASEM placement annotated. (b) Magnetic-actuated circuit breaker innards with solenoid and PASEM placement annotated.

which was plugged into the wall through a 20A power meter to provide reference power measurements. Lightbulb loads of various power ratings were switched on to load the breaker with different current magnitudes. The PASEM voltage and current sense signals were sampled with 16x averaging by an oscilloscope and subsequently processed in software to calculate real power. Figure 7 presents the results of this experiment, comparing the output of our PASEM sensor with the reference power meter. In this plot, the y-axis is a log scale, and measurement errors are less than 1% of full scale (1 kW) and typically less than 2% of measurement. From this plot, it is apparent that our sensing technique is very effective, showing strong correlation with a reference meter down to load power levels below 10W.

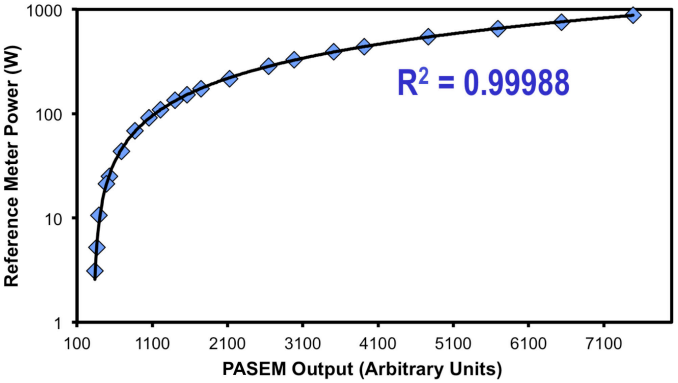

Fig. 7. PASEM output vs. reference plug-through power meter, showing great correlation to sub-10W load powers

B. Current to Voltage Phase Error Characterization

Maintaining a small phase error between current and line voltage signals is critical in a power meter design and leads to error in the calculation of real power dissipation. This test was performed with the entire system installed in a full circuit breaker panel, as shown in Figure 3. With a resistive load applied to a metered breaker, the phases of the digitized I_{sense} and $\alpha v_L(t)$ signals were compared over many 60 Hz cycles. Raw data shows a systematic phase error of $1.6°$, which was subtracted out as this can be accounted for in software when V_{sense} is shifted by (ideally) $90°$ to create $\alpha v_L(t)$. A histogram of the phase difference between the PASEM's digital current and voltage signals is shown in Figure 8. The standard deviation of the phase error is $3.4°$, which leads to 0.18% error in real power measurement for a resistive load (power factor $= 1$), and 3.05% error at power factor $= 0.9$. We believe that this is a promising result and is representative of the phase error introduced by all parts of the signal processing chain. The histogram appears to roughly follow a Gaussian shape, and the effective phase error between current and voltage signals can be reduced by averaging over multiple cycles, minimizing subsequent errors in real power estimation.

C. Performance with Non-Linear Loads

We measured the outputs of our PASEM sensor with a resistive load connected through a TRIAC dimmer to investigate how the sensor performs with a non-linear load. Figure 3 shows the test setup that was used for these measurements. The time domain waveforms measured during this test are shown in Figure 9a. These signals are shown with no averaging and were sampled at 1920 Hz using the PASEM's on-board microcontroller. It can be seen that abrupt changes in the circuit's current, introduced by the TRIAC, are tracked in the digitized I_{sense} signal. The frequency domain representation of the measured digital I_{sense} signal is also shown in Figure 9b. As expected, odd harmonics are prominent due to the TRIAC triggering events. This verifies the 960 Hz usable signal bandwidth resulting from our DC to $\approx$ 1 kHz analog front end, and on-board PASEM ADC's 960 Hz Nyquist frequency.

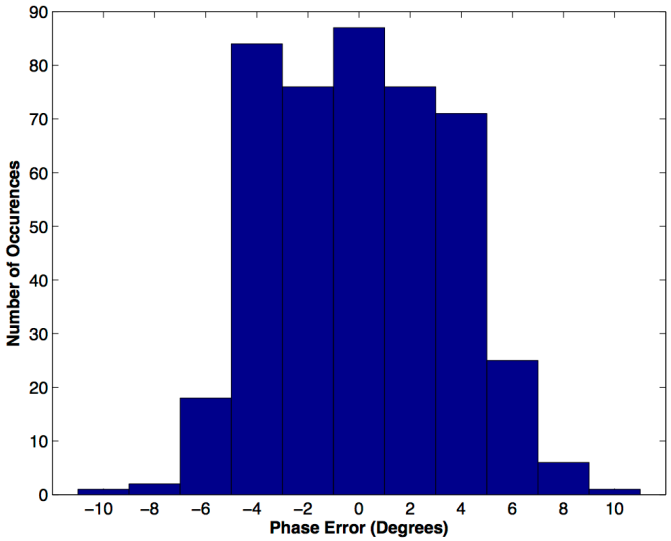

Fig. 8. Measured current-voltage phase difference for a resistive load.

D. In-Panel Crosstalk Characterization and Correction

Using the in-panel PASEM system installation shown in Figure 3, we characterized the signal crosstalk between neighboring circuits and sensors in the panel. With five sensors installed on consecutive breakers, the real power dissipation reported by all SEMs was monitored with a resistive load applied to only the middle circuit. The results of this experiment can be seen in Figure 10. This circuit breaker panel is wired in a split-phase 120V/240V configuration resulting in a $180°$ phase difference between the line voltage of adjacent circuits. This causes the alternating positive/negative power measurements visible in Figure 10, however, the sign of the measured real power at sensor *E* is opposite what is expected. We believe this is due to interference from other current-carrying conductors in the lower region of the breaker panel, highlighting a source of crosstalk besides the conductors inside the circuit breakers themselves. From this experiment, it is apparent that in-panel crosstalk from other conductors can lead to substantial errors in a circuit's real power estimation, and these effects must be accounted for to obtain valuable data in a real-world deployment.

Previous work in [9] showed that signals incident on the sensors from multiple conductors can be deconvolved to account for the current magnitude crosstalk between breakers. However, this technique requires applying a known load to every circuit in the panel to measure the cross-sensitivity matrix, which can be a difficult and time-consuming task in a full installation. We built upon the technique in [9] and created a method to account for crosstalk that operates on the PASEM real power measurements and does not require manually measuring the cross-sensitivity matrix. Our crosstalk cancellation method first uses the results from an electromagnetic simulation of a circuit breaker panel to estimate the cross sensitivity parameters and provide initial crosstalk mitigation. The types of circuit breakers in the panel should be known to improve the accuracy of the initial electromagnetic model. A statistical matching algorithm then monitors changes in mul-

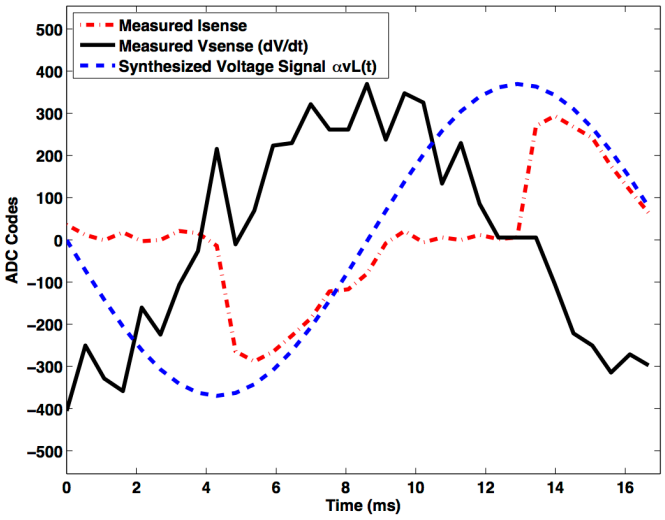

(a)

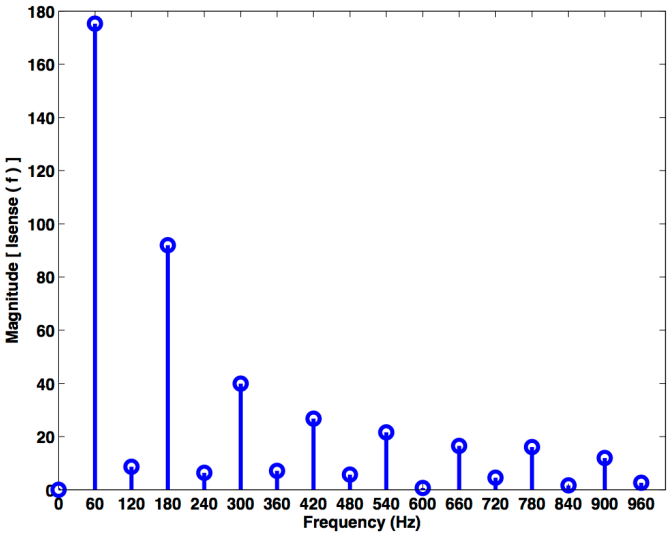

(b)

Fig. 9. (a) Sampled I_{sense}, V_{sense}, and phase-corrected line voltage signals for a TRIAC dimmer with resistive load. (b) FFT of sampled I_{sense} signal in (a).

tiple breaker signals simultaneously to improve the sensitivity matrix over time, further reducing errors due to the effects of nearby conductors on a circuit's power measurements.

To test the performance of our crosstalk cancellation algorithm, we used the installation shown in Figure 3 and applied a sequence of loads to circuits *B*, *C*, and *D*. The measured time-domain real power waveforms, with and without our crosstalk cancellation scheme enabled, are shown in Figure 11; the dashed traces represent the ideal values for the power of each circuit. Considering Figure 11a, very large errors are apparent without the crosstalk reduction technique applied. At some timepoints, negative power dissipation values are measured for circuits B and C. Using the same raw measured PASEM data and applying our crosstalk correction algorithm, the waveforms in Figure 11b are obtained. It can be seen that the correction algorithm drastically improves the real power estimates for all three circuits, as the measurements are much closer to the ideal values at all times. Even with this short < 15 minute time series, real power errors are under 5% for a majority of the time when the crosstalk mitigation algorithm is activated, and the error will decrease automatically as more data is gathered. We believe that this method of handling crosstalk is more practical for a real world deployment, due to a simpler installation procedure and continuously improving parameters.

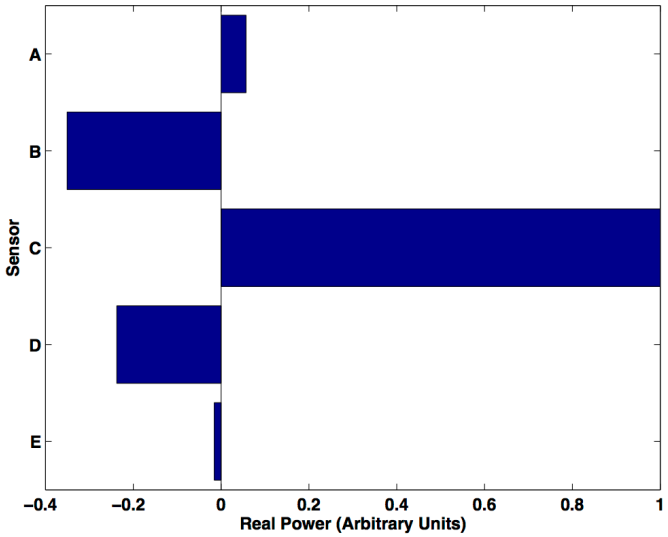

Fig. 10. Real power measured by neighboring breakers due to a load on the center breaker.

E. Long-Term Capacitive Voltage Sensing Accuracy

Shown in Figure 12 is the line to neutral voltage vs. time in a 480V, 3-phase system, measured both with our PASEM V_{sense} circuit and a standard, contact-based reference voltage measurement. Considering this plot, it is apparent that the voltage in a building can change over time and it is important for our PASEM device to track this variation correctly. Examining this data, the maximum error between our experimental sensor and the reference measurement is always less than 1% of the accepted measurement. The PASEM system is able to track these change in voltage, and the changes are automatically accounted for in the calculation of real power.

F. Residential Installation with Real Loads

Our PASEM system was installed on a single breaker in a home to test the sensor in a real-world environment with various load types and transients. The breaker panel used for this test was also outfitted with a TED 5000 whole house meter, serving as an accurate reference for calibration and measurement validation. During this experiment, the PASEM and wireless mote were powered by a 5V DC power supply plugged into a wall outlet near the circuit breaker panel. A laptop receiving wireless PASEM sensor data, executing Python DSP software, and uploading data to an SMAP server was placed in a room adjacent to the breaker panel.

The PASEM was installed on the dwelling's kitchen circuit, which contains multiple appliances. Calibration of the sensor

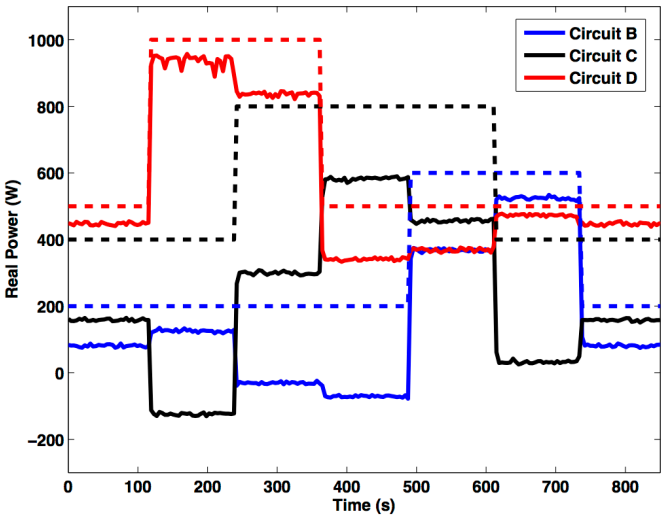

(a)

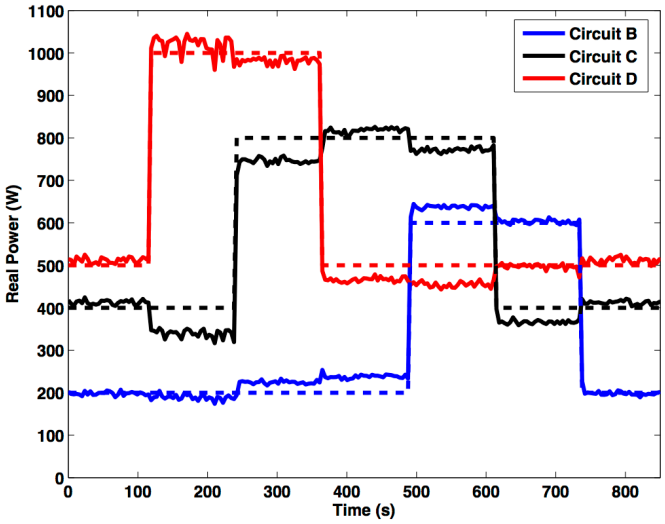

(b)

Fig. 11. Dashed traces represent ideal values. (a) Raw real power vs. time waveforms without crosstalk correction. (b) Real power vs. time waveforms with crosstalk correction algorithm applied.

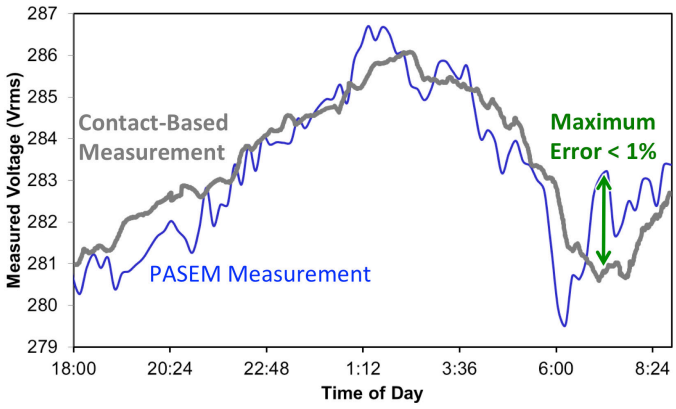

Fig. 12. Long-term, 480V 3-phase line-neutral voltage measurement. PASEM analog V_{sense} output vs. contact-based measurement.

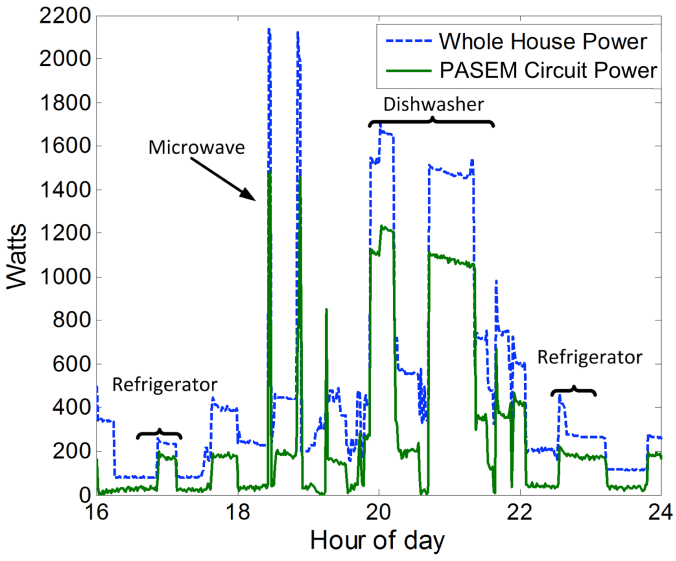

Fig. 13. Whole house and kitchen circuit PASEM meters' 8-hour energy data

was completed by plugging different resistive loads into a kitchen wall outlet (with other loads static), and monitoring changes in the output of the PASEM and TED meter. A plot of the power data from both the PASEM-metered kitchen circuit and the reference TED meter over a period of 8 hours is shown in Figure 13. It can be seen that the PASEM sensor is accurately measuring power for loads with non-unity power factor. Differences in the trends of the two curves shown are due to load changes on other circuits in the residence.

V. Conclusion

We have presented a new sensor system for building submetering at the circuit breaker panel that solves many issues inhibiting the widespread adoption of current technologies. With the measurements shown in this paper, we have shown that our sensor accurately measures real power with a 960 Hz usable bandwidth, and works well in a residential installation with various types of loads. A fundamental limitation is the low SNR provided by commercial Hall effect sensors at the magnetic field magnitudes of interest. To improve the SNR, averaging is used and this creates a tradeoff between measurement resolution and update frequency. We have also shown that crosstalk from nearby circuit breakers is significant, but these effects can be mitigated with intelligent algorithms that don't require extensive calibration by manually loading each circuit in the panel. Our submetering solution includes cost effective hardware that is suitable for installation without an electrician, and is easy to produce without an exotic manufacturing process. We estimate the installed cost of our system to be roughly 10 times lower than other available solutions. We hope that a future PASEM sensor design will enable installation with calibration that does not require loading *any* building circuits, resulting in another significant decrease in install time and complexity. Hopefully such a system can lead to the broad deployment of submetering in real buildings of all types.

ACKNOWLEDGMENT

The authors would like to thank Xavier Villajosana Guillen, Travis Massey, Richard Przybyla, and Pramod Murali for helpful discussions during this work.

REFERENCES

[1] Energy Information Agency, *Annual Energy Outlook 2012 Early Release*, www.eia.gov/forecasts/aeo/er/.
[2] National Science and Technology Council Committee on Technology, Subcommittee on Buildings Technology Research and Development, *Submetering of Building Energy and Water Usage*, 2011.
[3] J. Granderson, M. A. Piette, and G. Ghatikar, "Building energy information systems: user case studies," *Energy Efficiency*, vol. 4, no. 1, pp. 17–30, 2011.
[4] G. Sullivan, W. Hunt, R. Pugh, W. Sandusky, T. Koehler, and B. Boyd, "Metering best practices: A guide to achieving utility resource efficiency, release 2.0." Department of Energy Federal Energy Management Program, 2011.
[5] P. Henderson and M. Waltner, "Real-time energy management." Natural Resources Defense Council, 2013.
[6] Q. Xu, M. Seidel, I. Paprotny, R. White, and P. Wright, "Integrated centralized electric current monitoring system using wirelessly enabled non-intrusive ac current sensors," in *Sensors, 2011 IEEE*, 2011, pp. 1998–2001.
[7] Q. Xu, I. Paprotny, R. White, and P. Wright, "Energy submetering for circuit breaker panels using mems or mesoscale passive proximity current sensor," in *PowerMEMS 2010*, 2010.
[8] R. Send, Q. Xu, I. Paprotny, R. White, and P. Wright, "Granular radio energy-sensing node (green): A 0.56 cm3 wireless stick-on node for non-intrusive energy monitoring," in *Sensors, 2013 IEEE*, Nov 2013, pp. 1–4.
[9] Q. Xu, I. Paprotny, M. Seidel, R. White, and P. Wright, "Stick-on piezoelectromagnetic ac current monitoring of circuit breaker panels," *Sensors Journal, IEEE*, vol. 13, no. 3, pp. 1055–1064, March 2013.
[10] S. N. Patel, S. Gupta, and M. S. Reynolds, "The design and evaluation of an end-user-deployable, whole house, contactless power consumption sensor," in *Proceedings of the SIGCHI Conference on Human Factors in Computing Systems*, ser. CHI '10. New York, NY, USA: ACM, 2010, pp. 2471–2480. [Online]. Available: http://doi.acm.org/10.1145/1753326.1753700
[11] S. Dawson-Haggerty, X. Jiang, G. Tolle, J. Ortiz, and D. Culler, "sMAP: a simple measurement and actuation profile for physical information," in *Proceedings of the 8th ACM Conference on Embedded Networked Sensor Systems*, ser. SenSys '10. New York, NY, USA: ACM, 2010, pp. 197–210.

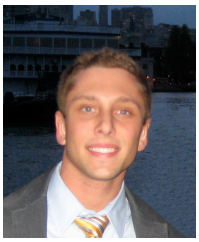

Michael C. Lorek (S'09) was born in Cleveland, OH and received the B.S. degree from Ohio University in Electrical Engineering in 2009. He is currently pursuing the Ph.D. degree in EECS at UC Berkeley under Prof. Kristofer S.J. Pister.

Michael has held various positions outside of academia, including internships at Advanced Micro Devices in 2007 and 2008, Qualcomm in 2011 and 2012, and a research fellowship at NIST in 2009. His current research interests include on-chip magnetic field sensing, energy harvesting interface circuits, and sensor node component integration.

Fabien Chraim (S'09) earned a Bachelor's degree with honors in Electrical and Computer Engineering from the American University of Beirut in 2009. He obtained an M.S. in Civil Systems Engineering from the University of California at Berkeley in 2010 after which, he joined the PhD program in Electrical Engineering and Computer Sciences. He is a student researcher working with Prof. Kristofer S.J. Pister at the Berkeley Sensor and Actuator Center since January 2010.

Kristofer S.J. Pister received his B.A. in Applied Physics from UCSD in 1986, and his M.S. and Ph.D. in Electrical Engineering from UC Berkeley in 1989 and 1992.

From 1992 to 1997 he was an Assistant Professor of Electrical Engineering at UCLA where he developed the graduate MEMS curriculum, and coined the phrase Smart Dust. Since 1996 he has been a professor of Electrical Engineering and Computer Sciences at UC Berkeley. In 2003 and 2004 he was on leave from UCB as CEO and then CTO of Dust Networks, a company he founded to commercialize wireless sensor networks. He participated in the creation of several wireless sensor networking standards, including Wireless HART (IEC62591), IEEE 802.15.4e, ISA100.11A, and IETF RPL. He has participated in many government science and technology programs, including DARPA ISAT and the Defense Science Study Group, and he is currently a member of the Jasons. His research interests include MEMS, micro robotics, and low power circuits.

Steven Lanzisera (S'02-M'09) received the Ph.D. degree in electrical engineering and computer sciences from the University of California, Berkeley in 2009. He was a test engineer with the Space Physics Research Laboratory from 1999 to 2002. At Berkeley he studied low-energy, networked technologies including the design of radios, communication protocols, and embedded systems.

In 2009 he joined Lawrence Berkeley National Laboratory, Berkeley, CA where he is Research Scientist and Principal Investigator of Applied Energy Sciences. His primary research areas involve new sensors and systems for the monitoring and control of energy using devices in buildings using new information technologies.